Automatic Reading of Electro-mechanical Utility Meters

Conference Paper · November 2013

DOI: 10.1109/MICAI.2013.28

Automatic Reading of Electro-mechanical Utility Meters

Ricardo Ocampo-Vega and Gildardo Sanchez-Ante *Senior Member, IEEE* and Luis E. Falcón-Morales
Tecnológico de Monterrey, Campus Guadalajara
Av. Gral. Ramón Corona 2514, Col. Nuevo México
Zapopan, Jalisco, 45201
Humberto Sossa
Instituto Politécnico Nacional-CIC
Av. Juan de Dios Batiz S/N, Gustavo A. Madero 07738
México, Distrito Federal, México

***Abstract*—Electro-mechanical meters are commonly used to measure the consumption of utilities. There are basically two kinds of analog meters: the ones that use rotary dials and the ones with pointer-type dials. Former approaches have dealt with the first kind of meters. Considering that reading the last ones can be confusing, in this work we introduce a methodology to enable the automatic reading of such devices. This methodology uses an image acquired with a smartphone and by applying a sequence of image processing functions finds and extracts the dials of such meters. Then identifies the position of the pointers and a clever implementation enables the reading. The proposed method was tested with a database, getting promising results. The database is composed with images taken under different light conditions, perspectives and angles.**

(a) Rotary-type dial set.

(b) Pointer-type dial set.

Fig. 1. Two types of dial utility meters.

I. Introduction

Meter readers are used worldwide to keep track of consumption of utilities such as water, gas and electricity. Although new digital meters are being installed recently, there is still an important number of analog meters. Some analog meters offer the readings using dials with numerals, like the one shown in Fig. 1(a). Others use pointer-type dials, like the one in Fig. 1(b). While reading the first kind of dials is straightforward, the correct reading of the second class is not that easy. It requires the application of several rules, that can be somewhat confusing for someone not familiarized with the process. In this work, we propose a methodology to extract the correct reading using as input an image of the dials. In particular, one of the main contributions of this work is that we deal with the problem of reading meters with pointer-type dials, while basically all of the related approaches are able to extract the reading from rotary-type dials. Another contribution is that we created an image database that incorporates images taken with smartphone cameras, under different illumination conditions, with varying orientations of the meter and even lacking information due to specular brightness, occlusions and other factors. This database was used to validate our approach.

The reminder of this paper is structured as follows. Section II reviews relevant work. Section III presents the methodology we propose to acquire and compute the reading of the dial meter. Section IV describes the experiments performed. We conclude this paper with a discussion on future work in Section V.

II. Previous Work

Most of the works reported are focused on the reading of images of rotary-numbers dials, like the one depicted in Fig. 1(a). One of the first works reported on the use of image processing to automate the reading of watt meters is reported in [1]. In such work, they report an automatic system based on image processing. There are three main components, one is a reading terminal that captures images of individual meters, then a computer called area concentrator and a main computer than receives the information of all the concentrators. Under this architecture, the reading terminal consists of a sort of video camera that takes pictures in real time and transmits them to the area concentrator. The area concentrator collect and store the information of a number of reading terminals, it is also the responsible of identify the numbers in the images representing the watt meters. As for the image processing in the area concentrators, it is important to mention that the meters they consider are the ones with digits representing the readings, not the one with dials. In a way, that problem is easier because once the area with the numerals is isolated, the problem consists basically in an optical character recognition problem. In a very related problem, the authors of [2] and

[3] propose an electronic device that has to be mounted to the meter. The device includes a camera, an array of LEDs to properly illuminate the meter and other components to digitally process the image and prepare it to be sent to a concentrator using ZigBee technology. The image processing procedure is divided into four steps including image preprocessing, target region positioning, character segmentation and character recognition. For this last step, they use a neural network. In [4], the authors focus their attention to water meters. Water meters usually include several pointers, located in four to five dials (sub-dials, actually). The methodology used by the authors require four big steps: 1) Image enhancement, 2) Tilt correction, 3) Print wheel location and 4) Sub-pointer location. Some of the algorithms used are Canny's edge detector to Fourier transform, centroid evaluation as other operations. The experimental results basically measure only whether the algorithm was able to accurately locate the dial pointer areas. There is no reading reported in that paper. However, in another work of the same group [5] more technical details are given. Again, the description is focused on the location and segmentation of all the dials in the image. The paper mentions that the algorithm can segment pointer images, but there is no information on extracting any number out of such images. The work reported in [6], the authors propose a system comprised of a wireless camera pointed at the meter to be read and a computer that receives and processes the image. The computer analyzes the image with pattern recognition technology to obtain the numbers. They perform image preprocessing, image segmentation (Otsu threshold method), and number recognition with a neural network. As with all the former cases, the image is one of a rotary-numbers dial. The work reported in [7] is also for the same kind of dials, but in this case they emphasize that their methodology can run on a handheld terminal. This could be interpreted like an efficient optical character recognition algorithm running on a handheld device. Also, the methodology considers that there are many variables that cannot be easily controlled when using such types of devices. Thus, the process involves a preprocessing phase with de-noising, binarization, distortion correction, segmentation and finally some operations to extract the numerals and perform number recognition.

There are also some patents in related topics. In [8] the inventors present an automated reader to monitor channels for gas, electricity and water utilities. It is a physical device that has to be installed at the site of a standard utility meter. The device described in [9] is also a circuitry to collect, calculate, store and display data correlative of the consumption of utility commodities. Finally, the patent we found closer to what we are describing here is the one in [10], where it is described a system for remote meter viewing and reporting. This system comprises a remote camera located at the meter. The camera scans the meter face, stores an image that is sent to a central computer and by using software to analyze the image, it can determine the consumption of the commodity, such as electricity. The way in which the information is extracted from the image is not described. The authors say that by using known image processing algorithms that can be done and in case that those algorithms are not able to recover the reading from the image, an exception processing is started, comprising an investigation of the cause of the corrupted image. Those descriptions are too generic to be directly implemented.

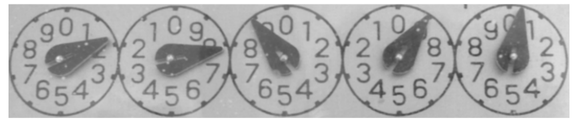

Fig. 2. Pointer-dials whose correct decimal reading corresponds to 17890

In contrast to [1], [4], [5] and [7] we report the performance of our method with images in real conditions; in such a way, we face challenges that arise when images taken outdoors are used, such as dealing with bright and shaded areas. Furthermore, we treat images taken at different positions, angles and perspectives; therefore, there are no restrictions regarding the position of the camera to the user. Also, the process described here does not require more intervention of the user other than taking the photo of the meter.

III. Methodology

The image in Fig. 2 shows a particular configuration of a dial meter. The reading, when performed by a human follows these guidelines:

1) Dials 1, 3 and 5 (counted left to right) rotate in clockwise direction and dials 2 and 4 rotate in counter-clockwise direction.
2) When a dial hand or pointer is between numbers, record the lower number. When the hand is between 9 and 0, record 9.
3) if the pointer is exactly on the borderline of two numbers, and the reading of the previous dial is between 0 and 5, then report the number corresponding to the borderline; otherwise, the preceding number must be chosen.
4) Report the numbers, left to right.

The meter reading for the example above is 17890.

To automate the process, the following steps are considered. The process starts with the acquisition of the image of the meter. To do that, the camera of a smartphone can be used. We assume that the pictures taken may be far from ideal, but we would like to prepare our system to be as reliable as possible. Then, some preprocessing of the images may be required. The second step will be the extraction of features that will allow for the segmentation of the image, and then the recognition of the digits. This process is illustrated in Fig.3.

A. Image Acquisition

The process starts with an image of the meter. We consider that images are of a quality given by the a smartphone camera. Although many of such devices have good resolution, their optics and software are not that robust. That means that images with exposition values not necessarily optimal or with blurry subjects are more or less common. Given that we could not find any publicly available database with meter images, we created one. Some of the images can be seen in Fig. 4. As

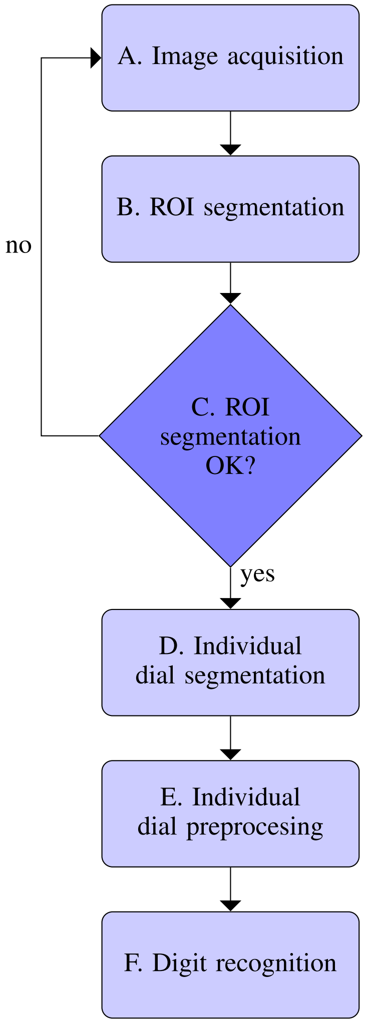

Fig. 3. Flowchart for our methodology.

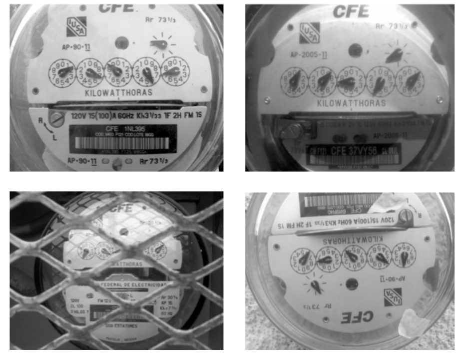

Fig. 4. Four images of our database. The first two are in better conditions than the last two.

(a) Image that shows how keypoints from the object are matched with keypoints of the scene.

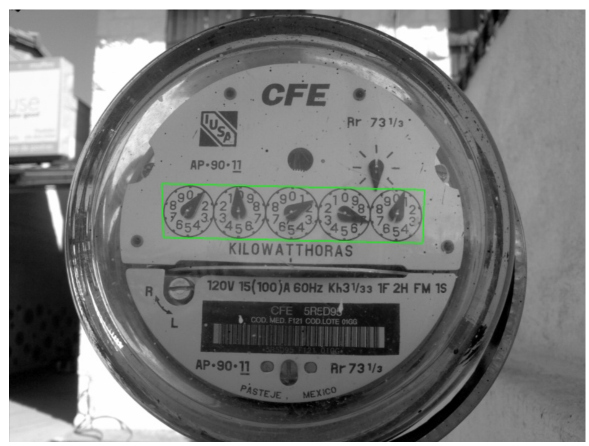

(b) Image obtained after segmentation of region of interest.

Fig. 5. Images derived from region of interest segmentation

it is possible to notice, some of them are quite clear, while others present elements that will definitively test how robust the algorithm is.

B. Segmentation of the Region of Interest

We use Scale-Invariant Feature Transform (SIFT) features [11] in order to extract an image with the dial set as shown in Fig. 1(b). SIFT is used because it performs reliable matching between different views of an object or scene. SIFT technique, in contrast to other methods, provides invariant features to image scale and rotation. Moreover, they are shown to provide robust matching across substantial range of affine distortion, change in 3D viewpoint, addition of noise, and change in illumination [11].

In this case, we will refer to the reference image Fig. 1(b) as object, and to the image in which we want to find the set of dials as scene (see Fig. 4). In order to extract the desired image, we matched the extracted features of the object and the extracted features of the scene using brute-force descriptor matcher. For each object's descriptors, the brute-force descriptor matcher finds the closest descriptor in the scene by trying each one until all the descriptors are compared. Fig. 5(a) shows the matches found with this technique.

In the matching process, there are keypoints that might be considered as outliers. Thus, the Euclidean distances for all matches were calculated in order to detect these outliers. The minimum Euclidean distance multiplied by a factor was considered as the borderline; all the matches that exceeded the

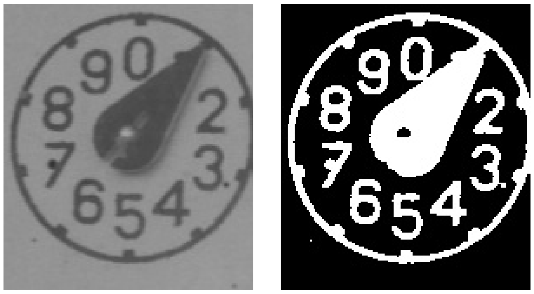

(a) Dial extracted. (b) Image after binarization.

Fig. 6. Images before and after using Otsu's thresholding.

0	0	0	0	0	0	1	0	0	0	0	0	0
0	0	0	0	0	0	1	0	0	0	0	0	0
0	0	0	0	0	0	1	0	0	0	0	0	0
0	0	0	0	0	0	1	0	0	0	0	0	0
0	0	0	0	0	0	1	0	0	0	0	0	0
0	0	0	0	0	0	1	0	0	0	0	0	0
1	1	1	1	1	1	1	1	1	1	1	1	1
0	0	0	0	0	0	1	0	0	0	0	0	0
0	0	0	0	0	0	1	0	0	0	0	0	0
0	0	0	0	0	0	1	0	0	0	0	0	0
0	0	0	0	0	0	1	0	0	0	0	0	0
0	0	0	0	0	0	1	0	0	0	0	0	0
0	0	0	0	0	0	1	0	0	0	0	0	0

(a) Structuring element of 13 $\times$ 13.

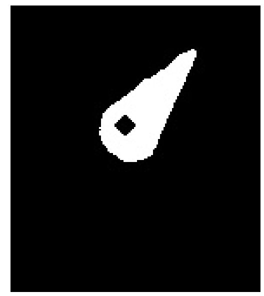

(b) Image after opening.

Fig. 7. Result after applying a morphological opening over Fig. 6(b).

borderline were considered as outliers. The factor mentioned before was calculated empirically. Fig. 5(b) shows a rectangle that was automatically obtained. The former processes were computed using OpenCVs implementation. Using the four points, we extract the rectangle and we divide it into five equal parts; therefore, it is possible to separate each of the pointers for further processing as shown in Fig. 6(a).

C. Region of Interest Validation

The expected shape of the segmented region of interest is a rectangle, but at most cases, a parallelogram is returned. We found that any form different to a parallelogram leads to an incorrect digit recognition. Therefore, we check if each angle formed by the four points of the region of interest exceed a threshold. This threshold is reckoned empirically.

D. Individual Dial Segmentation

Once the region of interest has been validated as a rectangle, in this step such geometric shape is divided into five rectangles. Each one of them encloses one of the circular dials.

E. Individual Dial Preprocessing

The next step is to segment the individual pointers. The image is binarized, resulting in a new image like the one shown in Fig. 6(a). After this, Otsu's thresholding method [12] is used given its simplicity. This method selects an optimal threshold by the discriminant criterion, to maximize the separability of the resultant classes in gray levels. Fig. 6(b) shows the resulting image after thresholding.

Mathematical morphology processing is necessary to extract the pointer, to erase the numbers and the circle that surrounds it. Mathematical morphology is defined by [13] as a tool for extracting image components that are useful in the representation and description of region shape, such as boundaries, skeletons, and the convex hull.

There are two fundamental operations of morphology: *erosion* and *dilation*. Erosion can be seen as a morphological filtering operation in which image details smaller than the structuring element are filtered from the image; on the other hand, dilation, unlike erosion, "grows" or "thickens" objects in a binary image; the specific manner and extent of this thickening is controlled by the shape of the structuring element [13]. *Opening* is an operation that generally smooths the contour of an object, breaks narrow isthmuses, and eliminates thin protrusions. The opening operation is conformed of eroding an image with a structuring element, followed by dilating the resulting image with the same structuring element.

Here we use the morphological techniques for filtering, thinning, and pruning the image obtained after binarizing the original image. After using an opening operation with the structuring element shown in Fig. 7(a). A binary image is obtained that contains just the pointer as shown in Fig. 7(b). This process is repeated for each of the five pointers of the electro-mechanical meter.

After the opening operation, an image that shows the pointer without undesirable noise is obtained. This pointer holds some characteristics, such as symmetry and a defined tip. In order to get an accurate reading, it is necessary to take advantage of these attributes.

F. Digit Recognition

For the purpose of getting a precise reading, it is needed to find an approach to find the next two points: 1) The tip and 2) The centroid of the pointer. The two points are needed in order to find the angle of the pointer with respect to the x-axis; consequently, this angle can be transformed into the individual reading (see Fig. 8).

The discrete computation of the centroid is given by

$$M_{pq} = \sum_x \sum_y x^p y^q f(x,y) \tag{1}$$

and the components of the centroid are

$$\overline{y} = M_{01}/M_{00} \quad (2)$$

$$\overline{x} = M_{10}/M_{00} \quad (3)$$

There are different options to locate the tip point. In our method, we find the pixel in the border of the binarized image such that maximizes the Euclidean distance between it and the centroid.

Finally, it is needed to calculate Eq. (4) and (5) in order to determine the angle between the x-axis and the line that is created joining the two points (tip and centroid). Fig. 8 shows the points found with Eq. (2) and (3) and the angle formed after drawing the line that passes through them.

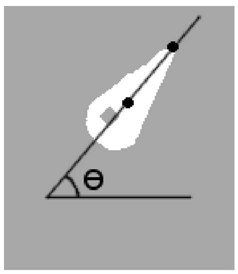

Fig. 8. Figure showing the tip, the centroid found, and the angle of the pointer.

Using just Eq. (4) it is not possible to read the pointer given the range of the function $\arctan$ that goes from $-\pi/2$ to $\pi/2$. This information describes just the position of the dial in the quadrant I and IV of the plane, hence, there isn't enough information. It is merely possible to read numbers from 0 to 4 using the available data; however, if we calculate the $\arcsin$ function then it is possible to know in which quadrant a pointer is, using the sign of ϕ. For Eq. (4) and (5), the subscripts c and t mean centroid and tip respectively.

$$\theta = \arctan\left(\frac{y_c - y_t}{x_c - x_t}\right) \quad (4)$$

$$\phi = \arcsin\left(\frac{y_c - y_t}{\sqrt{(y_c - y_t)^2 + (x_c - x_t)^2}}\right) \quad (5)$$

After calculating θ and ϕ, Table I is used to assign the corresponding reading.

TABLE I. READINGS REGARDING DIFFERENT ANGLES

Reading	θ	ϕ
0	$\pi/2 \geq \theta > 3\pi/10$	$\phi > 0$
1	$3\pi/10 \geq \theta > \pi/10$	$\phi > 0$
2	$\pi/10 \geq \theta > -\pi/10$	$\phi > 0$
3	$-\pi/10 \geq \theta > -3\pi/10$	$\phi < 0$
4	$-3\pi/10 \geq \theta > -\pi/2$	$\phi < 0$
5	$\pi/2 \geq \theta > 3\pi/10$	$\phi < 0$
6	$3\pi/10 \geq \theta > \pi/10$	$\phi < 0$
7	$\pi/10 \geq \theta > -\pi/10$	$\phi < 0$
8	$-\pi/10 \geq \theta > -3\pi/10$	$\phi > 0$
9	$-3\pi/10 \geq \theta > -\pi/2$	$\phi > 0$

IV. Experiments

A. Data Collection

The images used were collected without establishing a specific hour to take the pictures; on the contrary, they were taken at random hours of the day, so that, sun position varies and thus to get different scenarios. Because of the requirements of the image processing functions that we use, the pictures were taken with auto-focus, they were set to be black and white, and the size was fixed to 2 megapixel. A set of 141 images were gathered, and they are available for research purposes [14].

B. Metrics

We assess the algorithm using the following metrics, (1) number of bad segmentations, (2) number of false positives, and (3) elapsed time. The number of bad segmentations is the total images that once processed were rejected in the evaluation process. We consider a false positive as an incorrect digit extraction. The elapsed time is the total time it takes to complete the process from the acquisition of the first image to the digit recognition of the last image.

C. Results

The algorithms were run on a laptop computer i5 Intel processor at 2.4 GHz with 4Gb RAM running Arch-Linux. Given that we could not find other works for the same problem (extracting the reading from pointer-type meters), performing a comparison with other methods was not possible. However, we tested the performance varying the method used to segment the region of interest, which we believe is the critical step. For that purpose, we used SIFT as well as a combination of HARRIS/BRIEF. HARRIS [15] is used to detect keypoints and Binary Robust Independent Elementary Features (BRIEF) [16] extracts descriptors. SIFT does both.

Table II shows the results obtained after implementing SIFT and HARRIS/BRIEF. Using the image database that we created [14], we found that SIFT was faster and also that segmented better in comparison with HARRIS/BRIEF. Nevertheless, when the best pictures are selected, HARRIS/BRIEF seems to segment as good as SIFT but much faster (See Table III).

TABLE II. RESULTS USING SIFT/SIFT AND HARRIS/BRIEF WITH THE COMPLETE DATABASE

	SIFT/SIFT	HARRIS/BRIEF
Total of meters:	141	141
False positives (dials):	61	43
Bad segmentations:	31	67
% Bad segmentations:	22%	48%
% False positives:	11%	12%
Elapsed time (sec):	537.52	1351.34

The validation of the region of interest diminish the false-positives detected. We found that if the image is taken at a larger distance from the meter, the processing time increases, affecting more to HARRIS/BRIEF than to SIFT's method.

TABLE III. RESULTS USING SIFT/SIFT AND HARRIS/BRIEF WITH THE IMAGES IN GOOD CONDITIONS

	SIFT/SIFT	HARRIS/BRIEF
Total of meters:	36	36
False positives (dials):	13	19
Bad segmentations:	4	4
% Bad segmentations:	11%	12%
% False positives (dials):	8%	11%
Elapsed time (sec):	96.17	41.2

Also, we discovered that if the image is not well focused, the appropriate keypoints might not be detected.

We have to point out that the digit recognition step is particularly sensitive to big bright areas as well as big shade areas in the image.

V. CONCLUSIONS AND FUTURE WORK

After running the proposed method, we automatically extracted the readings of electro-mechanical meters using pictures that were taken under real conditions. Although many of the pictures in our database are in not good conditions, high level of accuracy can be achieved (92%). It should be pointed out that a good segmentation is particularly important to obtain good results.

In this case, the best keypoint detector and descriptor extractor was shown to be SIFT, even though the HARRIS/BRIEF combination achieves accurate results as well. The latter because when HARRIS/BRIEF combination is tested with pictures that present large areas of background, it takes longer time to detect keypoints, and it fails most of the time given this conditions.

Considering the steps of our method, many changes can be made in order to be more accurate with readings or to raise the number of segmented images. One of the possible variations in the code is the method used to extract the set of five dials.

Mathematical morphology is also a key process in order to get precise readings. As mentioned in Sect. III-E, defining an adequate structuring element is the hardest part of the opening operation; nevertheless, if this activity is carried on carefully then good results shall be accomplished.

ACKNOWLEDGEMENTS

The authors thank to Tecnológico de Monterrey, Campus Guadalajara under the program of Cátedras de Investigación, to Instituto Politécnico Nacional-CIC under project SIP 2013-1182, and to CONACYT under project 155014 for the economical support to carry out this research. We also thank all the reviewers for their valuable comments.

REFERENCES

[1] Shu, D., Ma, S., Jing, C.: Study of the automatic reading of watt meter based on image processing technology. In: 2nd IEEE Conference on Industrial Electronics and Applications, IEEE (2007) 2214–2217

[2] Zhao, L., Zhang, Y., Bai, Q., Qi, Z., Zhang, X.: Design and research of digital meter identifier based on image and wireless communication. In: International Conference on Industrial Mechatronics and Automation. (2009) 101–104

[3] Bai, Q., Zhao, L., Zhang, Y., Qi, Z.: Research of automatic recognition of digital meter reading based on intelligent image processing. In: 2nd International Conference on Computer Engineering and Technology (ICCET). Volume 5. (2010) V5–619–V5–623

[4] Zhang, Z., Li, Y.: Research on the pre-processing method of automatic reading water meter system. In: International Conference on Artificial Intelligence and Computational Intelligence. Volume 3. (2009) 549–553

[5] Zhang, Z., Li, Y., Yuan, W.: Research on pointer location of multi-pointer meter. In: IEEE International Conference on Automation and Logistics. (2009) 911–914

[6] Arun, S., Rao.M, V.: Implementation of image processing techniques in the automatic meter reading employed in critical and hazardous processes. International Journal of Computer Science and Information Security **9**(8) (2011) 165–170

[7] Lei, H., Zhang, P., Zeng, Q., Li, X.: Numeral recognition of power meter on a handheld terminal. In: Proceedings of the Third International Symposium on Electronic Commerce and Security Workshops. (2010) 76–79

[8] Shuey, K.C., Smith, K.J., Hemminger, R.C., Bragg, A.W.: Rf repeater for automatic meter reading system (1999) US Patent 5,874,903.

[9] Farnsworth, R.G., Robinson, P.B.: Automatic meter reading and control system (1983) US Patent 4,396,915.

[10] Gillberry, W.A.: System for remote meter viewing and reporting, Google Patents (1999) US Patent 5,870,140.

[11] Lowe, D.G.: Distinctive image features from scale-invariant keypoints. Int. J. Comput. Vision **60**(2) (2004) 91–110

[12] Otsu, N.: A threshold selection method from gray-level histograms. Systems, Man and Cybernetics, IEEE Transactions on **9**(1) (1979) 62–66

[13] Gonzalez, R.C., Woods, R.E.: Digital Image Processing (3rd Edition). Prentice-Hall, Inc., Upper Saddle River, NJ, USA (2006)

[14] Ocampo, R.: Pointer-type meters database. https://www.dropbox.com/sh/8ia1a9nd4qxznz4/vZl0G63P45 (2013) [Online; accessed 19-Sep-2013].

[15] Harris, C., Stephens, M.: A combined corner and edge detector. In: Alvey vision conference. Volume 15., Manchester, UK (1988) 50

[16] Calonder, M., Lepetit, V., Ozuysal, M., Trzcinski, T., Strecha, C., Fua, P.: Brief: Computing a local binary descriptor very fast. IEEE Transactions on Pattern Analysis and Machine Intelligence **34**(7) (2012) 1281–1298